Color Image Denoising Using Evolutionary Computation

Rastislav Lukac, Konstantinos N. Plataniotis, Anastasios N. Venetsanopoulos

Multimedia Laboratory, The Edward S. Rogers Sr. Department of Electrical and Computer Engineering, University of Toronto, Toronto, ON, Canada

Received 2 May 2005; accepted 21 December 2005

ABSTRACT: Noise suppression in multichannel data sets, such as color images, has drawn much attention in the last few years. An issue of paramount importance in designing color image filters is the determination of the coefficients that should be used to weight the inputs to the filter. In this study, we propose an evolutionary computation-based approach to select and optimize the coefficients in the class of weighted vector directional filters. Using a genetic algorithm, we were able to adapt the filter weights to match varying image and noise characteristics. Extended experimentation with realistic image processing applications, including television image enhancement and virtual restoration of artworks, indicates that the proposed filters are capable of removing noise while preserving chromaticity information, edges, and fine details, as well as structural image content.
 Int J Imaging Syst Technol, 15, 236–251, 2005; Published online in Wiley InterScience (www.interscience.wiley.com). DOI 10.1002/ima.20058

Key words: color image filtering; vector directional processing; genetic algorithm; constrained optimization

I. INTRODUCTION

In the last few years, evolutionary computation (EC) solutions (Man et al., 1999; Goldberg, 2002) have been applied to solve difficult optimization problems via simulated evolution. By repeatedly utilizing selection and reproduction principles to the population of individuals representing solutions to the problem, the evolutionary techniques evolve a satisfactory solution quickly and efficiently. Therefore, EC tools find applications in many problems ranging from telecommunication networks (Arabas and Kozdrowski, 2001), to fuzzy learning (Russo, 2000), to modeling (Fujiwara and Sawai, 1999; Chen et al., 2002), and data mining (Brameier and Banzhaf, 2001; Parpinelli et al., 2002), as well as image processing problems mostly related to gray-scale restoration (Hamid et al., 2003), feature extraction (Liu et al., 1997), and coding (Dasgupta et al., 2000). In this study, we intend to use genetic algorithm (GA) in color image filtering and enhancement applications (Lukac et al., 2005a). This choice is reasonable due to the fact that: (i) the intention of this experimentation is to obtain the globally optimal setting of the directional processing based vector filtering scheme considered, (ii) GAs are relatively easy to implement, (iii) the optimization problem defined over the vectorial inputs is complex, and (iv) GAs work well in noisy conditions.

Color image processing (Plataniotis and Venetsanopoulos, 2000; Lukac et al., 2005a) has gained much interest over the past few years since color information conveys information needed for image understanding and object recognition. Humans and image processing systems use color information to sense the environment. The human eye recognizes thousands of different colors and uses the information to identify visual objects and understand the environment. Color image systems are used to capture and reproduce the scenes that humans see. However, as imaging systems are built using optical, electronic, and chemical components, the process is not without problems. Random variations in the sensor readings make the recorded values different from the ideal ones, introducing errors and undesirable side effects in the subsequent stages of the image processing process (Fig. 1). Noise affects the perceptual quality of the image decreasing not only the appreciation of the image but also the performance of the task for which the image was intended. Therefore, noise filtering and image enhancement are essential part of any image processing system, whether the processed information is utilized for visual interpretation or for automatic analysis (Lukac et al., 2005a).

Image filtering can be divided into: (i) reconstruction filtering, and (ii) enhancement filtering. In general, reconstruction filters attempt to suppress and remove image corruption noise by utilizing prior knowledge on the type of image degradation. Image enhancement techniques process an image so that the final results are more suitable than the original image for a specific application.

Numerous filtering techniques have been proposed to date for multichannel image processing. With regards to the multichannel nature of the color image, these techniques can be classified as component-wise techniques (Rantanen et al., 1992; Zheng et al., 1993) and vector techniques (multichannel or multivariate) methods (Plataniotis and Venetsanopoulos, 2000; Lukac et al., 2004d; Lukac et al., 2005a).

Component-wise techniques are the early methods of multichannel image processing. These methods are direct extensions of the traditional approaches developed for gray-scale images (Pitas and Venetsanopoulos, 1990; Mitra and Sicuranza, 2001) and operate on color channels separately (Rantanen et al., 1992; Zheng et al.,

Correspondence to: Rastislav Lukac; E-mail: lukacr@ieee.org, web: http://www.dsp.utoronto.ca/~lukacr

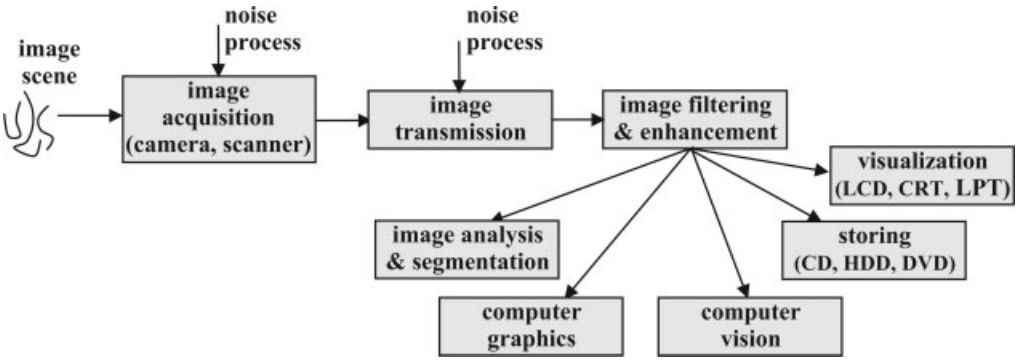

Figure 1. Image processing chain.

1993). Since separate processing discards inherent correlation between color channels, component-wise filtering often results in color artifacts (Lukac et al., 2005a).

It has been widely recognized (Trahanias et al., 1996; Plataniotis et al., 1999; Smolka et al., 2003) that vector processing of color images is a more effective way to filter out noise and to enhance color images. Each pixel of an image is represented by three values, which can be treated as a vector. Thus, any color image can be considered a vector field where each vector's direction and length are related to the pixel's color characteristics and influence significantly its perception by the human observer (Lukac et al., 2005a). The vector filtering procedure can be described according to some distance criterion, which is applied to the set of input vectors inside a processing window.

The vector median filter (VMF) (Astola et al., 1990) is the most commonly used member of the vector filtering family (Plataniotis and Venetsanopoulos, 2000; Vardavoilia et al., 2001; Lukac et al., 2005a). To quantify relative magnitude differences of the input samples, the VMF filtering class utilizes the well-known Euclidean distance or the generalized Minkowski metric. Because vectors, which diverge greatly from the data population, usually correspond to maximum aggregated relative magnitude differences, the VMF output is the sample that minimizes the aggregated Euclidean distance to the input vectors. To improve the detail-preserving characteristics of the VMF, the basic idea has been modified in designs of the extended VMF (Astola et al., 1990), weighted VMF (Viero et al., 1994; Lucat et al., 2002; Lukac et al., 2003a; Lukac et al., 2004c), extended weighted VMF (Viero et al., 1994), outlier rejection VMF schemes (Lukac, 2003; Smolka et al., 2003), vector filters based on the reduced ordering according to the reference point in the vector space (Tang et al., 1995), gradient-based design (Lin and Hsueh, 2000), VMF-rational filters (Khriji and Gabbouj, 1999), fuzzy vector filters (Tsai and Yu, 2000; Lukac et al., 2005b), and noise filtering techniques based on the digital path approach (Szczepanski et al., 2003).

However, it has been observed that the filtering techniques taking into the account vectors' magnitude often produce color outputs with chromaticity problems. To alleviate such problems, a new type of multichannel filters was proposed (Trahanias et al.; 1996). The so-called vector directional filter (VDF) family operates on the direction of the image vectors, aiming to eliminate vectors with atypical directions in the vector space. To achieve its objective, the VDF utilizes the angle between the image vectors to order vector inputs inside a processing window (Plataniotis and Venetsanopoulos, 2000; Tang et al., 2001; Lukac et al., 2005a). As a result of this process, a set of input vectors with approximately the same direction in the vector space is produced as the output set. The idea of directional processing of color images is employed by the basic vector directional filter (BVDF) (Trahanias et al.; 1996), generalized vector directional filter (GVDF) (Trahanias et al.; 1996), double window GVDF (GVDF-DW) structures (Plataniotis and Venetsanopoulos, 2000), spherical median filter (SMF) (Plataniotis and Venetsanopoulos, 2000), and fuzzy VDF (Plataniotis et al., 1999; Lukac et al., 2005b). The directional distance filter (DDF) (Karakos and Trahanias, 1997) and vector median-vector directional hybrid filters (HVF) (Gabbouj and Cheickh, 1996) combine the properties of both VMF and VDF designs. Recently developed weighted vector directional filters (WVDF) (Lukac, 2004; Lukac et al., 2004a) extend the flexibility of the VDF based designs and provide a powerful color image filtering tool capable of tracking varying signal and noise statistics.

This study focuses on GA optimization of the WVDF filters. The work extends the preliminary results presented in conference

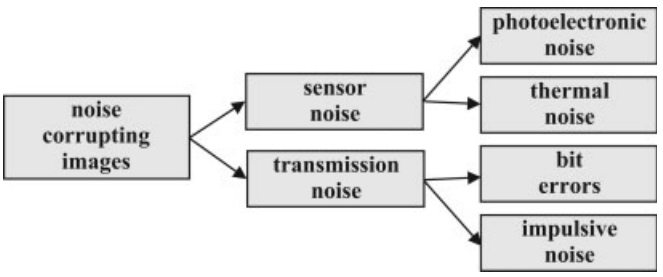

Figure 2. Noise frequently introduced into the image.

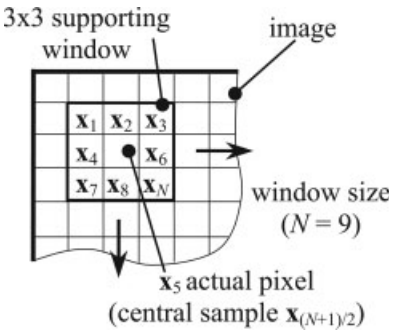

Figure 3. Sliding filtering window ensuring the stationarity of the processes generating the image.

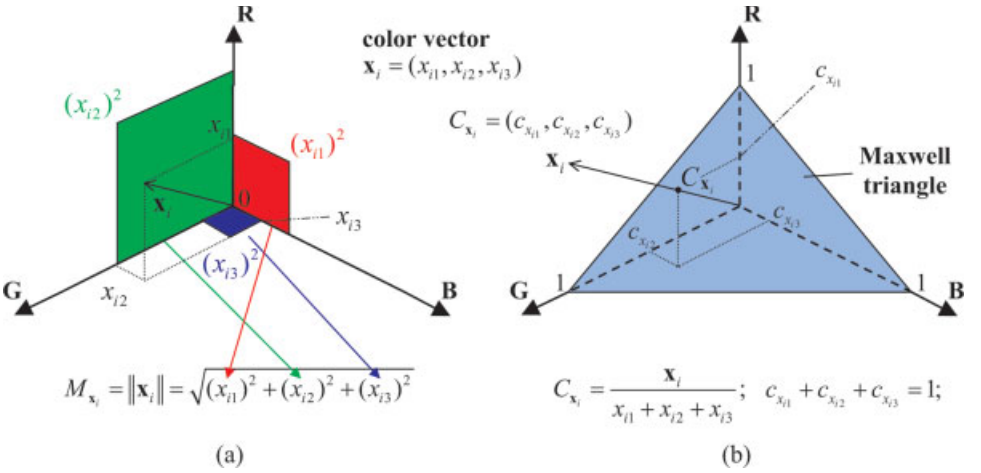

Figure 4. Basic parameters related to the color vector $\mathbf{x}_i = [x_{i1}, x_{i2}, x_{i3}]$: (a) magnitude (brightness) M_{x_i}, (b) direction (chrominance) illustrates as the point C_{x_i} defined on the Maxwell triangle. [Color figure can be viewed in the online issue, which is available at www.interscience.wiley.com]

publications (Lukac et al., 2003b,c; 2004b). Mathematical approaches to the WVDF optimization problem have been addressed in (Lukac et al., 2004a). Unfortunately, these methods based on least mean absolute (LMA) or least mean square (LMS) adaptation algorithms usually do not converge to a globally optimal weight vector (Lukac et al., 2004a,c). This can result in worse WVDF detail-preserving characteristics. Since the GA, a biologically oriented computational technique, searches the whole solution space (in a sufficiently large time or number of generations), it provides the globally optimal (or very close) solution. Using the GA, we avoid situations when, due to the wide search space and the amount of data to be processed, other optimization techniques may fail to find the optimal solution. We will show that the proposed genetically optimized WVDF filter achieves excellent results in terms of commonly used objective image quality criteria and can outperform the state-of-the-art color image filters as well as local adaptation based WVDF approaches introduced in (Lukac et al., 2004a). The efficiency of the proposed method will be examined using well-known test images as well as real images of digitized artworks and television images.

The rest of the study is organized as follows. In Section II, the formulation of the problem is introduced and color image filtering fundamentals are presented. A generalized class of WVDF filters operating on the directionality of color vectors is described in Section III. Optimal design features are discussed in Section IV. Section V focuses on the GA optimization of the WVDF filters. Motivation, design characteristics, and variations of the proposed method are discussed in detail. In Section VI, the proposed solution is analyzed in terms of optimization and parameters used. Proposed optimized filters are tested in a variety of noise corrupted test images as well as television images and digitized images of fine arts. Conclusions are offered in Section VII.

II. PROBLEM FORMULATION

Let us consider a $K_1 \times K_2$ color image $\mathbf{x} : Z^2 \rightarrow Z^3$ representing a two-dimensional matrix of three-component samples (pixels) $\mathbf{x}_i = [x_{i1}, x_{i2}, x_{i3}]$. Components x_{ik}, for $k = 1, 2, 3$ and $i = 1, 2, \ldots, K_1K_2$, represent the color channel values quantified into the integer domain Z. The process of displaying an image creates a graphical representation of the image matrix where the pixel values represent particular colors. It should be emphasized that color pixels are multichannel signals commonly termed as color vectors (Plataniotis and Venetsanopoulos, 2000; Lukac et al., 2005a). Therefore the term color vector is used throughout the paper.

Noise introduced into color images (Fig. 2) is present in the form of artifacts significantly deviating from neighboring pixels. This results in color distortions to which the human visual system is very sensitive (Faugeras, 1979). In many practical applications, color images are corrupted by additive noise. The most commonly used model is defined (Plataniotis and Venetsanopoulos, 2000; Lukac et al., 2005a) as follows

$$\mathbf{x}_i = \mathbf{o}_i + \mathbf{v}_i, \tag{1}$$

where $\mathbf{x}_i$ represents the observation (noisy) sample, $\mathbf{o}_i = [o_{i1}, o_{i2}, o_{i3}]$ is the desired (noise free) sample, $\mathbf{v}_i = [v_{i1}, v_{i2}, v_{i3}]$ is the vector describing the noise process, and i characterizes the spatial position of the samples in the image. Note that $\mathbf{v}_i$ can describe both signal-dependent and independent noise.

The most popular color filtering techniques operate on some type of sliding (moving, running) window $W = \{\mathbf{x}_i \in Z^2;\ i = 1, 2, \ldots, N\}$ of finite odd size N, (Fig. 3). The filtering operation usually

```
Inputs:  NumberOfRows × NumberOfColumns noisy image
         Window size N
         Moving window spawning the input set {x_1, x_2, ..., x_N}
         Weight vector w = {w_1, w_2, ..., w_N}
Output:  NumberOfRows × NumberOfColumns image

For a = 1 to NumberOfRows
  For b = 1 to NumberOfColumns
    Determine the input set W(a,b) = {x_1, x_2, ..., x_N}
    For i = 1 to N
      For j = 1 to N
        Compute the angle A(x_i, x_j)
      End
      Compute the sum β_i = w_1 A(x_i, x_1) + w_2 A(x_i, x_2) + ... + w_N A(x_i, x_N)
    End
    Sort β_1, β_2, ..., β_N to the ordered set β_(1) ≤ β_(2) ≤ ... ≤ β_(N)
    Apply the same ordering to x_1(β_1), x_2(β_2), ..., x_N(β_N)
    Store ordered sequence as x_(1) ≤ x_(2) ≤ ... ≤ x_(N)
    Let the filter output y(a,b) = x_(1)
  End
End
```

Figure 5. Algorithm of the WVDF filtering.

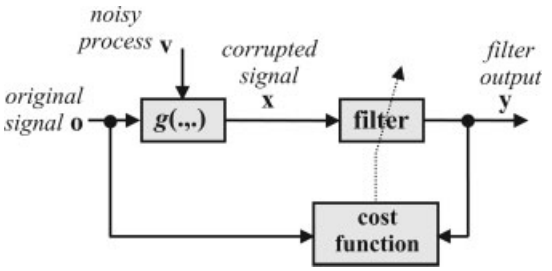

Figure 6. Optimal filter designed under the minimization of the cost function.

affects one image sample—usually the sample $\mathbf{x}_{(N+1)/2}$ placed in the center of the window—at a time, changing its value by applying a function on the local neighborhood area $\{\mathbf{x}_1, \mathbf{x}_2, \ldots, \mathbf{x}_N\}$. This window operator slides over the image to affect individually all the image pixels (Lukac et al., 2005a). The localized nature of the operator allows for the minimization of the local distortion and ensures the stationarity of the processes, including the noise and blurring characteristics.

Following the tristimulus theory of color, each color pixel $\mathbf{x}_i$ inside the supporting window is treated as a three-dimensional vector in the RGB color space (Wyszecki and Stiles, 1982; Lukac et al., 2005a). As such, it is uniquely defined (Fig. 4) by its magnitude $M_{\mathbf{x}_i} : Z^2 \rightarrow R^+$

$$M_{\mathbf{x}_i} = \|\mathbf{x}_i\| = \sqrt{(x_{i1})^2 + (x_{i2})^2 + (x_{i3})^2} \tag{2}$$

and direction $C_{\mathbf{x}_i} : Z^2 \rightarrow T$ with coordinates

$$C_{x_{ik}} = \frac{x_{ik}}{x_{i1} + x_{i2} + x_{i3}}, \quad \text{for } k = 1, 2, 3 \tag{3}$$

defined on Maxwell triangle T^2, where $c_{x_{i1}} + c_{x_{i2}} + c_{x_{i3}} = 1$.

On the basis of the magnitude of color vectors, filtering techniques process the image according to its brightness, whereas operating on the directionality of the color inputs focus on the chrominance properties of the input vectors (Plataniotis and Venetsanopoulos, 2000; Lukac et al., 2005a). Since a vector's direction corresponds to its color chromaticity, filtering techniques operating on the directional domain of color images preserve their chromaticity. Since the human visual system is sensitive to changes in color and edge information (indication of the shape of objects in the image), color chromaticity preservation along with the noise attenuation and detail preserving capabilities are fundamental properties required in many applications (Lukac et al., 2005a), such as television image denoising, virtual restoration of artworks, satellite image processing, old movie restoration, and surveillance. Note that false colored and blurred edges introduced as a result of inappropriate filtering significantly degrade the quality of the perceived image. From an application point of view, the introduction of false edges and color shifts is considered to be more problematic than the presence of the noise.

III. WEIGHTED VECTOR DIRECTIONAL FILTERS

The recently introduced WVDF filters (Lukac et al., 2004a) employ nonnegative real weighting coefficients $w_1, w_2, \ldots, w_N$ associated with the input vectors $\mathbf{x}_1, \mathbf{x}_2, \ldots, \mathbf{x}_N$. These filters output the color vector $\mathbf{y} = \mathbf{x}_i \in W$, which minimizes the aggregated weighted angular distance to other samples inside W:

$$\mathbf{y} = \arg \min_{\mathbf{x}_i \in W} \sum_{j=1}^{N} w_j \, A(\mathbf{x}_i, \mathbf{x}_j), \tag{4}$$

where

$$A(\mathbf{x}_i, \mathbf{x}_j) = \arccos\left(\frac{\mathbf{x}_i, \mathbf{x}_j}{\|\mathbf{x}_i\|\|\mathbf{x}_j\|}\right) \tag{5}$$

$$= \arccos\left(\frac{x_{i1}x_{j1} + x_{i2}x_{j2} + x_{i3}x_{j3}}{\sqrt{x_{i1}^2 + x_{i2}^2 + x_{i3}^2}\sqrt{x_{j1}^2 + x_{j2}^2 + x_{j3}^2}}\right), \tag{6}$$

represents the angle between two color vectors $\mathbf{x}_i = [x_{i1}, x_{i2}, x_{i3}]$ and $\mathbf{x}_j = [x_{j1}, x_{j2}, x_{j3}]$.

This angular minimization approach is useful for directional data, such as color data. It has been proven that, in the case of color images, filtering schemes based on directional processing of color images may achieve better performance in terms of the color chromaticity (direction of color data) preservation than approaches operating on the vectors' magnitude (Nikolaidis and Pitas, 1998).

The output of the WVDF filter is determined using the algorithm summarized in Figure 5. Let us consider the aggregated weighted distance β_i associated with the input color vector $\mathbf{x}_i$:

$$\beta_i = \sum_{j=1}^{N} w_j \, A(\mathbf{x}_i, \mathbf{x}_j) \quad \text{for } i = 1, 2, \ldots, N. \tag{7}$$

The ordered sequence of $\beta_1, \beta_2, \ldots, \beta_N$ is given by $\beta_{(1)} \leq \beta_{(2)} \leq \cdots \leq \beta_{(N)}$. Assuming that the ordering of β_i terms implies the same ordering for the original set $\mathbf{x}_1, \mathbf{x}_2, \ldots, \mathbf{x}_N$, the ordered

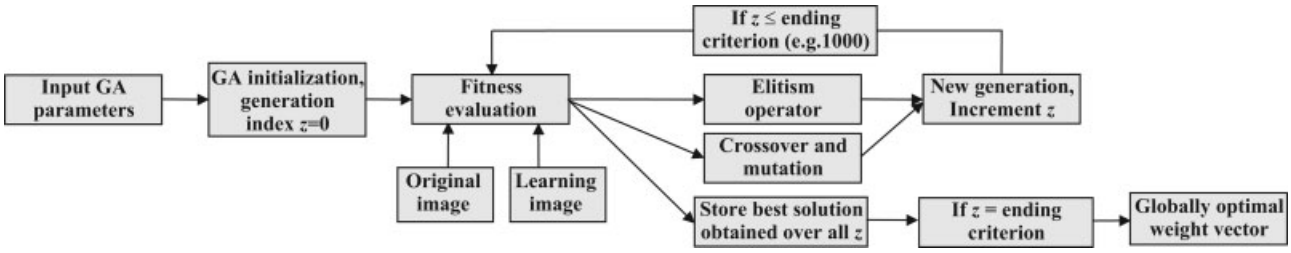

Figure 7. Block scheme of the GA optimization of the WVDF weighting coefficients.

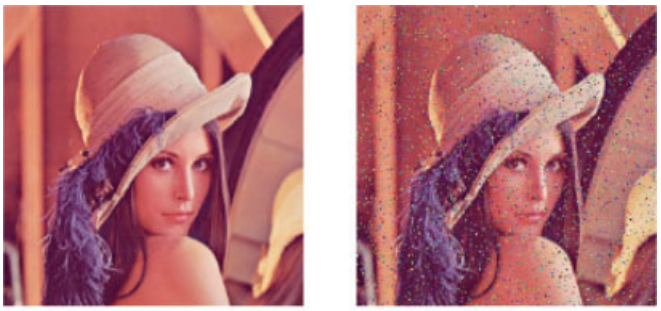

Figure 8. Test images serving as desired signal and training set, respectively: (a) original image Lena, (b) image corrupted by 10% impulsive noise ($p_v = 0.10$). [Color figure can be viewed in the online issue, which is available at www.interscience.wiley.com]

sequence $\mathbf{x}_{(1)} \leq \mathbf{x}_{(2)} \leq \cdots \leq \mathbf{x}_{(N)}$, where $\mathbf{x}_{(i)}$ is associated with $\beta_{(i)}$, can be obtained. In this case, the WVDF output is defined as the lowest order-statistics $\mathbf{x}_{(1)}$, which is equivalent to the sample minimizing earlier definition (4). From this algorithm, it is evident that the WVDF output is restricted to be the sample of the input set W and thus, it can never introduce a novel outlying vector. In addition, the WVDF output $\mathbf{y}(\mathbf{w}, W)$ is a function of the weight vector $\mathbf{w} = [w_1, w_2, \ldots, w_N]$ and it can be expressed as the sample $\mathbf{y} \in W$ minimizing $F(\mathbf{y}) = \Sigma_{j=1}^{N} w_j \, \mathrm{A}(\mathbf{y}, \mathbf{x}_j)$. Then, the following statements can be declared:

- The WVDF filter has N independent parameters $w_1, w_2, \ldots, w_N$ described by the weight vector $\mathbf{w}$.
- If the vectorial set W appear constantly in the WVDF input, the WVDF output $\mathbf{y}(\mathbf{w},W)$ depends only on the weight vector $\mathbf{w}$.
- The WVDF output corresponds to one of the local minimums of $F(\mathbf{y})$.

IV. OPTIMAL WVDF DESIGN

Each set of weighting coefficients represents a specific filter, which can be used for specific purposes. Using the optimization scheme (Fig. 6), the weighting coefficients can follow the statistics and structural content of desired signal and be adapted in the required manner. It will be shown that WVDF filters optimized for the removal of impulsive noise and the preservation of the color/structural information are sufficiently robust and do not necessitate additional optimization or weight vector adaptation in order to perform the task in other images where the corrupting noise, although varying in the amount and appearance, is impulsive in the nature. Moreover, we will demonstrate that WVDF filters optimized using the test images and noise approximations, can be used to remove outliers and noise impairments in real, nonsimulated applications such as television image denoising and virtual restoration of artworks. Note that these real images contain numerous noise impairments including low-amounts of additive Gaussian-type noise (e.g., thermal noise). In both applications, image filtering is of paramount importance, and the use of the proposed WVDF filters is highly suggested due to their excellent color/structural preserving characteristics.

The objective of the filtering operator is to accurately determine the unavailable color vector $\mathbf{o}$ given its noisy observation $\mathbf{x}$. To measure the similarity between the original vector and the obtained, filtered vector $\mathbf{y}$, a number of different objective measures can be utilized (Plataniotis and Venetsanopoulos, 2000). One of the most popular is the Minkowski family of metrics defined by

$$\|\mathbf{o} - \mathbf{y}\|_L = \left(\sum_{k=1}^{3} |o_k - y_k|^L \right)^{1/L}, \tag{8}$$

where L denotes the norm parameter, e.g., the city-block distance ($L = 1$) or Euclidean distance ($L = 2$), and o_k and y_k are the k-th elements of the original color vector $\mathbf{o}$ and the filter output $\mathbf{y}$, respectively.

In all optimal schemes discussed in this work, a loss function, which depends on the noiseless input vector and its filtered estimate, is used to penalize errors during the procedure. Following standard practice, it is only natural to assume that if one penalizes estimation errors through a loss function then the optimum filter is that function of the measurements which minimizes the average (expected) loss (Principe et al., 1999). For example, $E\{(\mathbf{o}-\mathbf{y})^2\}$, which corresponds to an average error measured using the Euclidean distance, is commonly used to derive filters operating under the additive Gaussian noise assumption. The selection-type filters are primarily focusing on removing outliers and impulsive noise in color images. Therefore, the average loss is defined using the absolute error $\|\cdot\|_1$ as follows:

$$E\{\|\mathbf{o} - \mathbf{y}\|_1\} = \frac{1}{K_1 K_2} \sum_{i=1}^{K_1 K_2} \|\mathbf{o}_i - \mathbf{y}_i(\mathbf{w}, W)\|_1, \tag{9}$$

where $\mathbf{y}_i(\mathbf{w}, W)$ denotes the WVDF output, which is considered to be the estimate of the original, noise free, color vector $\mathbf{o}_i$.

Ignoring the normalization factor in (9), the optimal WVDF can be obtained by minimizing the absolute error accumulated over all

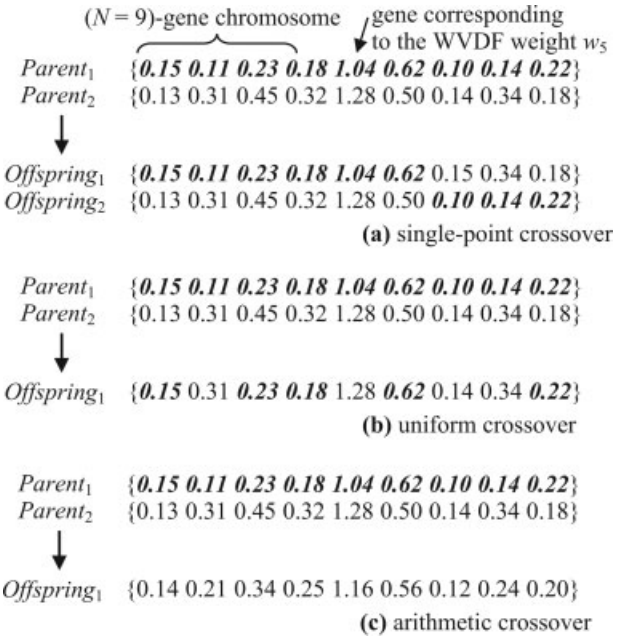

Figure 9. Crossover operator: (a) single-point crossover, (b) uniform crossover, (c) arithmetic crossover.

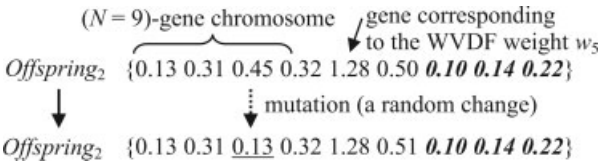

Figure 10. Mutation operator defined by the probability p_m introduces a random change into the chromosome.

possible signal locations $i = 1, 2, \ldots, K_1K_2$. This forms a WVDF cost function defined as follows:

$$J_{\mathrm{WVDF}}(\mathbf{w}) = \sum_{i=1}^{K_1K_2} \|\mathbf{o}_i - \mathbf{y}_i(\mathbf{w}, W)\|_1. \tag{10}$$

Enforcing the constraint of nonnegative weights in order to keep the aggregated distance (7) positive, the above optimization problem can be re-written as an optimization problem with inequality constraints:

$$\begin{aligned} &\text{minimize } J_{\mathrm{WVDF}}(\mathbf{w}) \\ &\text{subject to } w_i \geq 0, \quad \text{for } i = 1, 2, \ldots, N. \end{aligned} \tag{11}$$

V. GA OPTIMIZATION

In general, the WVDF optimization problem may be solved using a wide range of possible methods, but it is difficult to determine, analytically, the optimal one. The previously developed WVDF optimization framework (Lukac et al., 2004a) utilizes local adaptation based on linear and sigmoidal approximations of the sign function. It has been proven that these methods cannot converge to a globally optimal weight vector $\mathbf{w}$. Under certain application conditions, this restricts WVDF's detail-preserving characteristics. Since GA-based methods search the entire solution space (given sufficiently large processing time or number of generations), they can potentially provide a globally optimal (or very close) solution.

GA optimization approaches belong to the field of biologically oriented computational techniques (Goldberg, 1989). The GA is useful in applications, when other optimization techniques may fail to find the optimal solution due to the wide search space and the amount of data to be processed. Moreover, analytically oriented methods require the exact specification of the initial conditions—a difficult task in most practical applications.

GA optimization (Fig. 7) differs from traditional search algorithms due to the utilization of multiple candidate solutions (Man et al., 1999). Each candidate solution is represented by the so-called individual, a data structure that contains two parts, the so-called chromosome and fitness. A set of individuals constitutes a population, whose size N_p remains unchanged during the entire searching process. Note that small N_p leads to premature convergence upon a sub-optimal solution, whereas for too large N_p, GA tends to converge slower upon a solution. To avoid premature convergence caused by a small population size, $N_p = 120$ (i.e., 120 real-coded chromosomes) is utilized in this study.

A. Chromosome Representation. Based on nonnegative, real weighting coefficients, the candidate solutions—WVDF weight vectors—are represented by real-coded chromosomes. For the constraint optimization problem of (11), a real-coded chromosome representation has the advantage of being closer to the way candidate solutions are described in the application. Therefore, real chromosome coding is more appropriate, compared to binary coding, for the problem under consideration. In real-coded chromosomes, each variable of the chromosome is represented by one gene. In the WVDF optimization, each individual represents the weight vector $\mathbf{w}$ and each gene corresponds to the weighting coefficient $w_i \in \mathbf{w}$, for $i = 1, 2, \ldots, N$. Thus, chromosomes contain N genes corresponding to the N real-valued WVDF weights. Since each real-valued weight vector can be normalized into the unity space, it is reasonable to set the boundaries of the search space to $0 \leq w_i \leq 1$, for $i = 1, 2, \ldots, N$.

B. Training Set. To solve the optimization problem of (11), the utilization of a pair of original and corrupted (training set) images (Fig. 8) is required. In this study, the commonly used color image Lena serves as the original, training signal. This image is corrupted by impulsive noise following the additive model of (1) with the

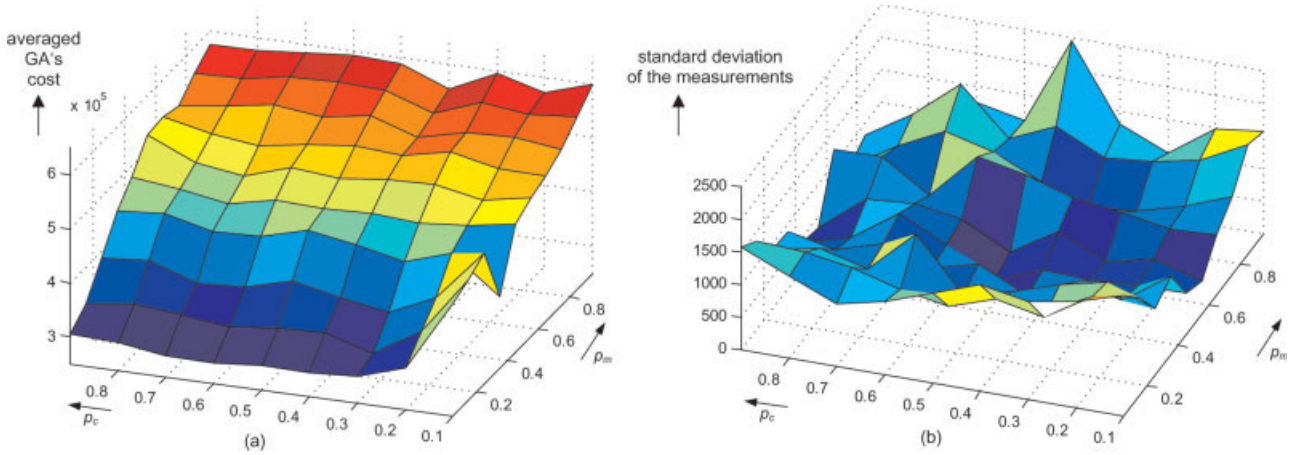

Figure 11. GA efficiency related to the WVDF optimization depending on crossover p_c and mutation p_m probabilities: (a) GA's cost function J_{GA} averaged over 20 runs, and (b) the corresponding standard deviation of the measurements. [Color figure can be viewed in the online issue, which is available at www.interscience.wiley.com]

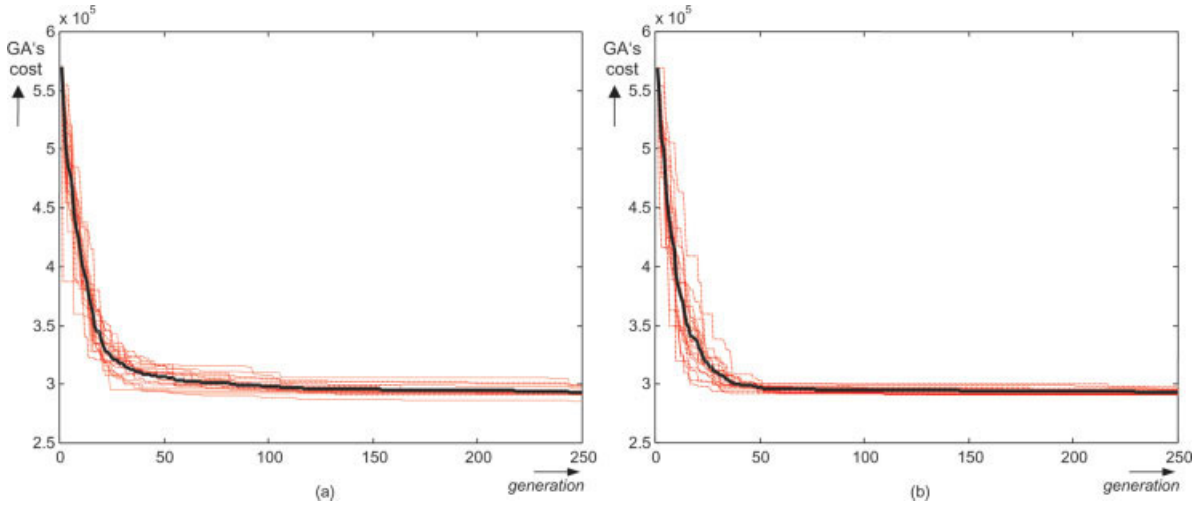

Figure 12. Convergence of the GA-WVDF optimization expressed through the GA's cost J_{GA} for $p_c = 0.7$ and $p_m = 0.05$ depending on the number of generations: (a) single-point crossover and Gaussian mutation, (b) arithmetic crossover and Gaussian mutations. Note that the dotted lines represent the cost of the individual runs, whereas emphasized lines represent the interpolated values. [Color figure can be viewed in the online issue, which is available at www.interscience.wiley.com]

noise component $\mathbf{v}_i$ defined as follows:

$$\mathbf{v}_i = \begin{cases} \mathbf{v}_i & \text{with probability } p_v \\ 0 & \text{with probability } 1 - p_v \end{cases} \tag{12}$$

where p_v is a corruption probability (also termed as the percentage number of corrupted pixels). The impulse $\mathbf{v}_i$ is independent from pixel to pixel making $\mathbf{x}_i$ of (1) a vector exhibiting much larger and/or smaller amplitude characteristics at least in one of the components, compared to those of the neighboring samples.

C. Fitness Function and GA's Cost. During the searching process, the GA requires a quality criterion, which is used to evaluate the generated solutions (individuals). The measure of the individual quality is known as a fitness value (Man et al., 1999). Based on their fitness, individuals are enforced to create offspring.

With respect to the optimization problem described in (11), achieving the output image for all individuals (solutions in forms of weight vectors $\mathbf{w}$), fitness values ξ_j corresponding to the individuals I_j, for $j = 1, 2, \ldots, N_p$, are given, similar to (Hamid et al., 2003), as follows:

$$\xi_j = 1 - \frac{\mathrm{MAE}_j}{\mathrm{MAE}_{\max}}, \tag{13}$$

where $\mathrm{MAE}_{\max}$ is the maximum possible mean absolute error (MAE) for the image (i.e., $\mathrm{MAE}_{\max} = 255$ in the case of 8 bits per channel representation), and MAE_j denotes the MAE value corresponding to the solution I_j. The MAE is defined as:

$$\mathrm{MAE} = \frac{1}{3K_1K_2} \sum_{k=1}^{3} \sum_{i=1}^{K_1K_2} |o_{ik} - y_{ik}|, \tag{14}$$

where $\mathbf{o}_i = [o_{i1}, o_{i2}, o_{i3}]$ is the original pixel, $\mathbf{y}_i = [y_{i1}, y_{i2}, y_{i3}]$ is the filtered pixel, i is the pixel position in a $K_1 \times K_2$ color image and k characterizes the color channel.

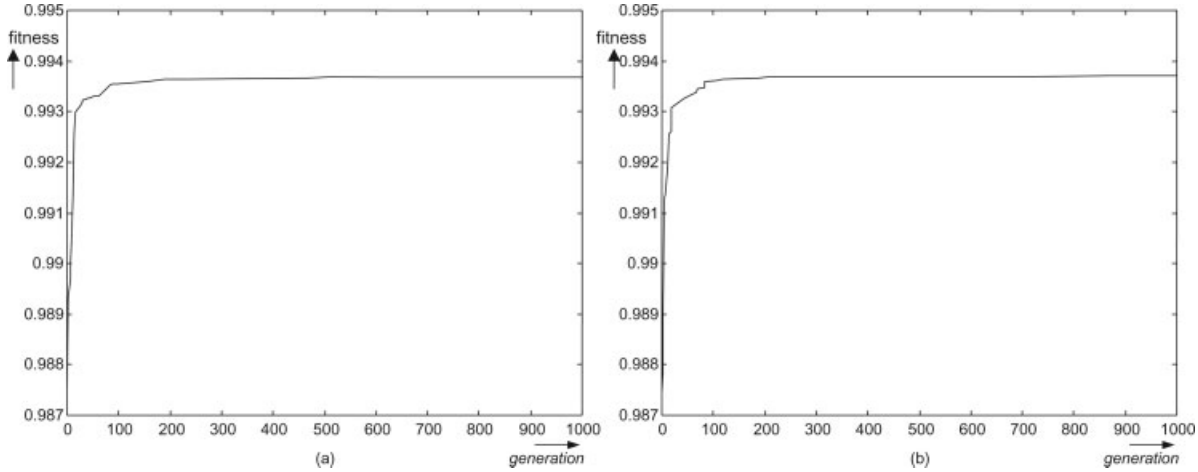

Figure 13. Maximum fitness depending on the number of generations for $p_c = 0.7$ and $p_m = 0.05$: (a) single-point crossover and Gaussian mutation, (b) arithmetic crossover and Gaussian mutation.

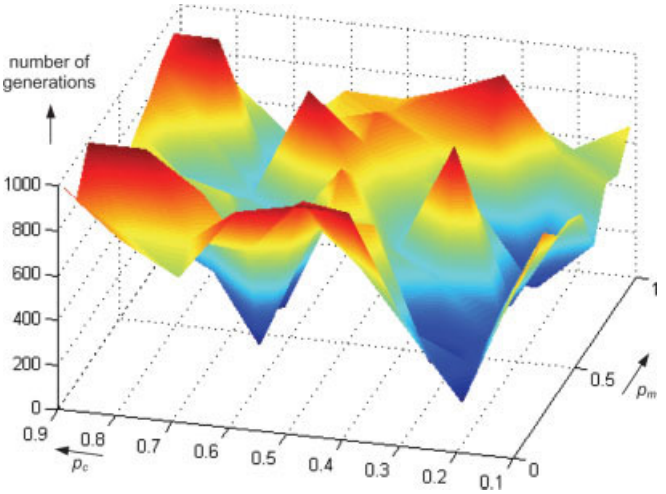

Figure 14. The number of the generations at which the final best solution obtained (within 20 runs) was reached versus the GA parameters p_c and p_m. [Color figure can be viewed in the online issue, which is available at www.interscience.wiley.com]

The earlier defined fitness values measure how close the solution is to the ideal solution. Individuals associated with large fitness values are capable of restoring quite accurately the processed image. Solutions associated with low-fitness values produce images, which deviate significantly from the in-accessible original.

It should be mentioned that the fitness values can be defined in many ways utilizing numerous image quality measures listed in (Avcibas et al., 2002). Following the traditional practice of image quality evaluation in the area of color image processing (Plataniotis and Venetsanopoulos, 2000; Lukac et al., 2004c), the mean square error (MSE) defined as

$$\mathrm{MSE} = \frac{1}{3K_1K_2}\sum_{k=1}^{3}\sum_{i=1}^{K_1K_2}(o_{ik}-y_{ik})^2, \tag{15}$$

and/or the normalized color difference (NCD) criterion (Plataniotis et al., 1999) defined by

$$\mathrm{NCD} = \frac{\sum_{i=1}^{K_1K_2}\sqrt{\sum_{k=1}^{3}(\bar{o}_{ik}-\bar{y}_{ik})^2}}{\sum_{i=1}^{K_1K_2}\sqrt{\sum_{k=1}^{3}(\bar{o}_{ik})^2}}, \tag{16}$$

may be considered as an alternative. While both MAE and MSE are defined in the RGB domain, the NCD criterion in 16) is defined in the CIE LUV color space, where $\bar{\mathbf{o}}_i = [\bar{o}_{i1}, \bar{o}_{i2}, \bar{o}_{i3}]$ and $\bar{\mathbf{y}}_i = [\bar{y}_{i1}, \bar{y}_{i2}, \bar{y}_{i3}]$ are the vectors representing respectively the RGB vectors $\mathbf{o}_i$ and $\mathbf{y}_i$ in the CIE LUV color space with the white reference point D65 (Wyszecki and Stiles, 1982). Thus, the NCD is useful for evaluating the color chromaticity differences between the color vectors and allows us to quantify the error in the uniformly perceived color space (Plataniotis and Venetsanopoulos, 2000). On the other hand, MAE and MSE are commonly accepted in the image processing community as the measures of signal-detail preservation and noise-attenuation, respectively. Although all aforementioned error criteria will be used in the sequence to quantify the difference between the original and filtered (or noisy) images, due to the simplicity of the implementation the fitness values of (13) are used here to guide the GA-WVDF optimization process.

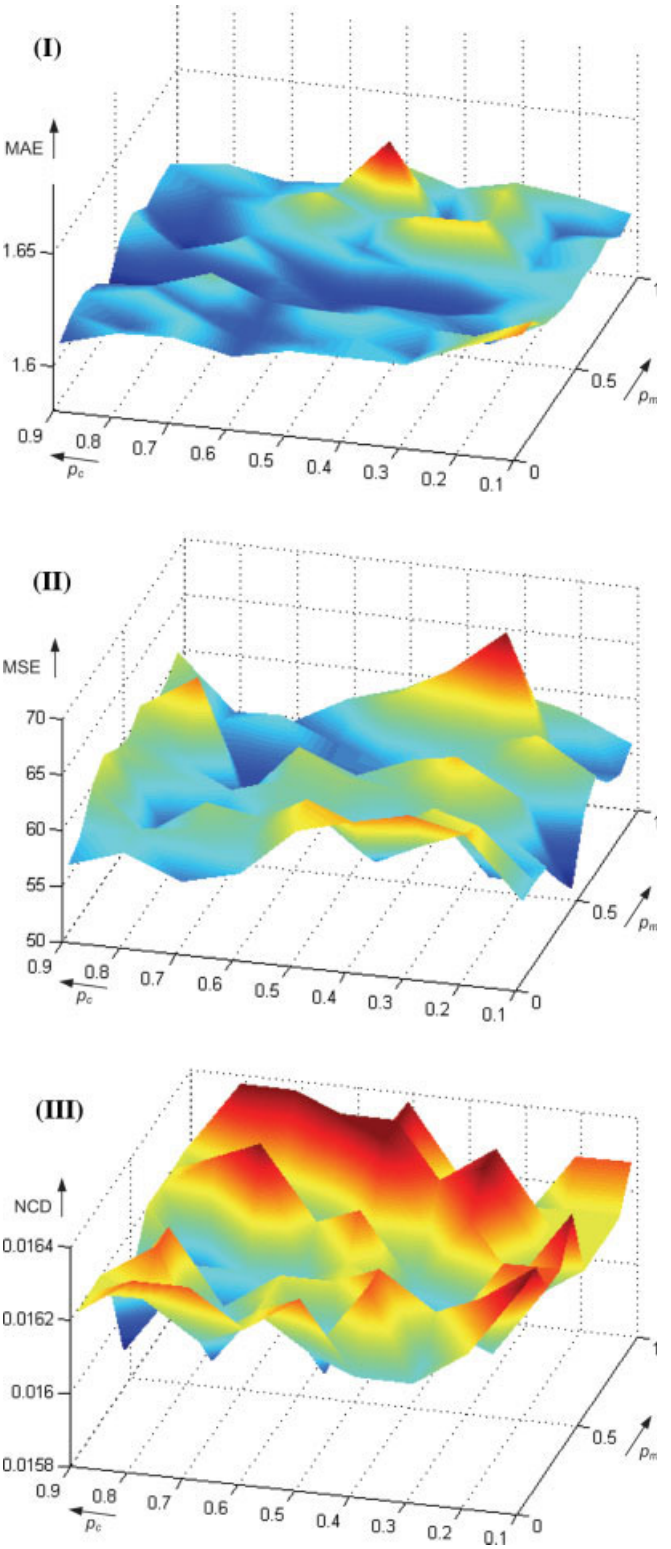

Figure 15. Appropriateness of the best solution expressed using the image quality criteria averaged over 20 runs. [Color figure can be viewed in the online issue, which is available at www.interscience.wiley.com]

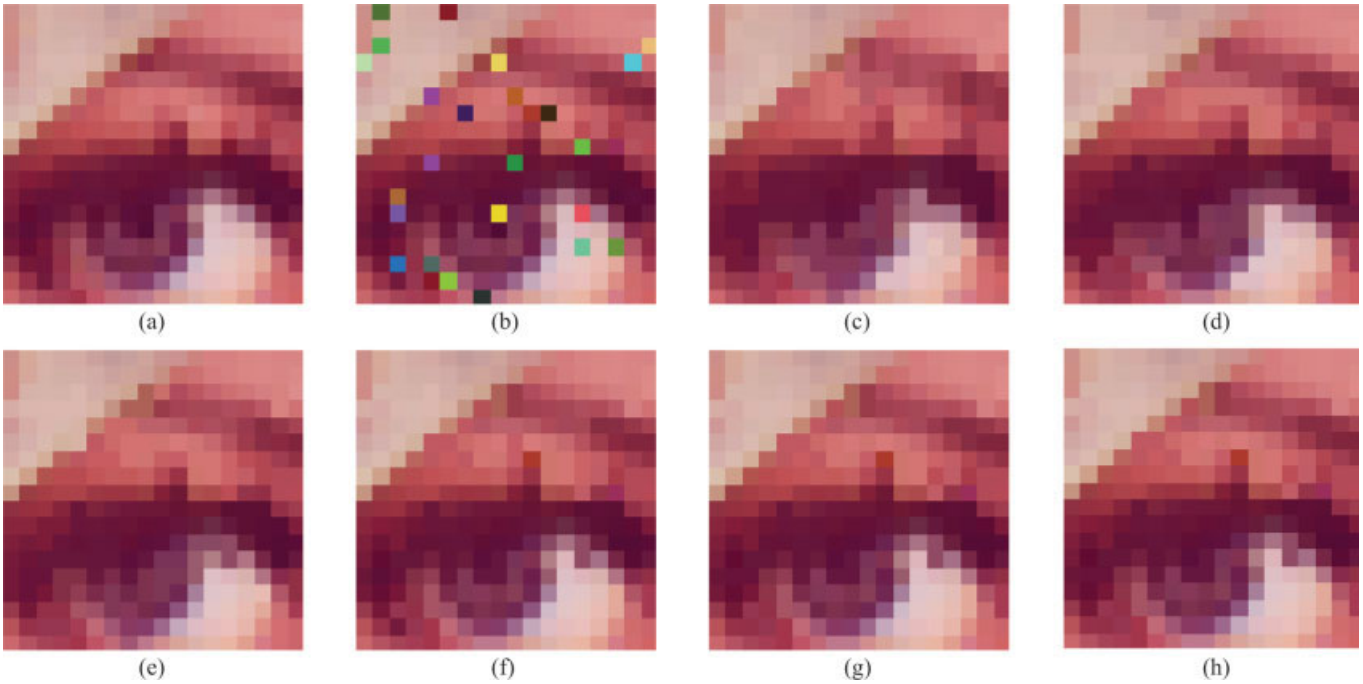

Figure 16. Zoomed parts of images achieved during the GA training: (a) original image, (b) image corrupted by 10% impulsive noise ($p_v = 0.10$), (c) 1st generation with MAE = 3.203, MSE = 53.9, NCD = 0.0332, (d) 3rd generation with MAE = 2.724, MSE = 64.3, NCD = 0.0283, (e) 10th generation with MAE = 2.398, MSE = 51.5, NCD = 0.0247, (f) 87th generation with MAE = 1.646, MSE = 62.8, NCD = 0.0166, (g) 217th generation with MAE = 1.619, MSE = 55.7, NCD = 0.0164, (h) 466th generation with MAE = 1.606, MSE = 55.2, NCD = 0.0162. [Color figure can be viewed in the online issue, which is available at www.interscience.wiley.com]

Assuming that $\mathbf{w}^j = [w_1^j, w_2^j, \ldots, w_N^j]$ is the weight vector corresponding to the individual I_j, for $j = 1, 2, \ldots, N_p$, the GA-WVDF optimization problem is expressed as:

$$\begin{aligned} &\text{minimize } J_{\text{GA}} = \tfrac{1}{N_p}\sum_{j=1}^{N_p} J_{\text{WVDF}}\left(\mathbf{w}^j\right) \\ &\text{subject to } w_i^j \geq 0, \text{ for } i = 1, 2, \ldots, N, \end{aligned} \tag{17}$$

where J_{GA} is the GA's cost function and

$$J_{\text{WVDF}}\left(\mathbf{w}^j\right) = \sum_{i=1}^{K_1 K_2} \left\|\mathbf{o}_i - \mathbf{y}_i\left(\mathbf{w}^j, W\right)\right\|_1. \tag{18}$$

is the cost function of the individual I_j. Visual inspection of (17) suggests that GA minimizes the error defined over the entire population. Therefore, it is reasonable to conclude that given sufficiently large number of generations, the obtained population will contain numerous acceptable solutions (Goldberg, 1989).

D. Genetic Operators. Based on an individual's fitness, the selection operator is used to select the parents from the current population of solutions in order to produce offspring. The chance of selecting an individual increases with its fitness. GA solutions strive to make compromises between selective pressure and diversity (Leung et al., 2001; Bosman and Thierens, 2003). Based on the setting of the initial parameters, the user can tune this trade-off and boost GA performance. To keep the selection process simple, a tournament selection is usually employed (Man et al., 1999). This selection mechanism compares a randomly constituted set of current individuals and selects the individual with the best fitness. The repeated process results in a second parent selection. Note that the selective pressure of this approach increases with the size N_s of the randomly constituted sets. In this study, we will make use of uniformly distributed, randomly generated, N_s.

Another genetic operator is the crossover and the corresponding crossover probability p_c. This operator creates offsprings by mixing and recombining the chromosomes of selected parents (Man et al., 1999; Leung et al., 2001). Figure 9a illustrates the traditional, single point crossover, which randomly selects a point of the crossover and replaces the genetic information of parents chromosomes after this point. Figure 9b illustrates a uniform crossover, in which the

Table I. Obtained weight vectors normalized according to their corresponding maximum values.

	Weighting Coefficients								
WVDF Type	w_1	w_2	w_3	w_4	w_5	w_6	w_7	w_8	w_9
LWVDF	0.3919	0.4634	0.3774	0.3766	1.0000	0.3824	0.3625	0.4624	0.3928
SWVDF	0.1920	0.4688	0.2771	0.2449	1.0000	0.2913	0.1838	0.5668	0.1602
Proposed $\mathbf{w}_1$	0.1763	0.2536	0.1574	0.1969	1.0000	0.1676	0.2240	0.2462	0.2176
Proposed $\mathbf{w}_2$	0.1526	0.2610	0.2007	0.2059	1.0000	0.1992	0.2115	0.2581	0.1435
Proposed $\mathbf{w}_3$	0.1719	0.3106	0.2248	0.2297	1.0000	0.2130	0.2125	0.3246	0.1817

Table II. Standard deviation corresponding to the weight vectors w_2 and w_3 (listed in Table 1) obtained through averaging of 1800 measurements (only winning chromosomes).

	Weighting Coefficients								
WVDF Type	w_1	w_2	w_3	w_4	w_5	w_6	w_7	w_8	w_9
$\mathbf{w}_2$	0.0354	0.0209	0.0322	0.0422	0.0525	0.0350	0.0325	0.0192	0.0338
$\mathbf{w}_3$	0.1148	0.1762	0.1180	0.1390	0.0600	0.1422	0.1084	0.1861	0.1495

value of each gene of an offspring is randomly taken form either parent. Figure 9c shows an arithmetic crossover, where the offspring is obtained by averaging the genes of the parent chromosomes. Note that sophisticated EC tools use special crossover operators that create offspring statistically located in proportion to the difference of the parents in the search space (Beyer and Deb, 2001). It should be emphasized that the weighting coefficients represent the degree to which each input vector contributes to the filter output. Therefore, the use of the single-point crossover preserves part of the weights' setting, transferring the sequences of weights from the best parents to offsprings during evolution. This is very important from an image processing point of view since the offspring are allowed to share the detail-preserving and noise-attenuating characteristics of the parents. Although this choice often slows down the convergence process compared to that noticed using the traditional arithmetic crossover, the new populations contain a large number of useful individuals. On the other hand, the use of the arithmetic crossover in the GA-WVDF optimization process unifies solutions to the weight vector corresponding to the best fitness. However, it is known that many, although seemingly different weight vectors, can produce similar, if not identical, outputs in the selection-type based nonlinear filters. By exchanging the sequence of the weights (genes) through the use of a single-point crossover, less uniform populations and more interesting filtering settings can be obtained.

Mutation operators are referenced via the mutation probability p_m. This operator (Fig. 10) is used to introduce small random information to the offspring. Note that mutation can potentially affect more than one gene of the chromosome, because each gene is mutated with the same probability p_m. The mutation operator can be implemented in many ways, for example (Goldberg, 1989; Man et al., 1999) (i) a uniform mutation replaces a gene with a random number from the interval specified for a given position in the chromosome, (ii) a Gaussian mutation adds to a gene a Gaussian distributed random value, (iii) a boundary mutation, which replaces a gene with the maximum or the minimum value currently used in the offspring representation. Since the mutation operator supports diversity, p_m should be set to a small value in order to obtain a practical convergence rate (Goldberg, 1989). In this study, the commonly accepted Gaussian mutation was used mainly due to the fact that the operator usually introduces only small changes in an individual. We allow up to six genes in each chromosome to be affected by the mutation operator. Both crossover and mutation probabilities p_c and p_m will be the subject of heuristic analysis provided in Section VI.

It is evident that because of recombining and mutation, duplicate individuals representing the same solutions may be produced. To avoid premature convergence and to increase the efficiency, any duplicate individuals should be eliminated from the pool of candidates.

Two other operators employed in our solution are the so-called generation gap (or subpopulation) and elitism operators. Both are determined by setting r_g (for generation map) and r_e (for elitism operator) to a real number between 0 and 1. Thus, r_g multiplied by N_p represents the fraction of the current population (usually the individuals with the worst fitness) which is to be replaced by the offspring. On the other hand, the elitism parameter r_e multiplied by N_p denotes the fraction of the best individuals, which will appear unchanged in next population. In this study, we employ an elitism operator defined by $r_e = 0.1$. Therefore, the individual with the best fitness reported during evolution corresponds to an optimal solution.

VI. APPLICATION TO COLOR IMAGES

In this section, the performance of the GA-WVDF filters is evaluated in the most important area of multichannel processing, namely color image filtering. The results presented in this paper were obtained with a 3×3 square window (i.e., $N = 9$) shown in Figure 3.

First, the GA efficiency is tested using the original image Lena (Fig. 8a) and its noisy version (Fig. 8b) in order to optimize the WVDF weights for an impulsive noise removal task. The performance characteristics of GA-WVDF optimization are evaluated using the GA's cost function, fitness values, and conventional color image error measures (MAE, MSE, and NCD). Note that the single-point crossover, Gaussian mutation, and an optimization boundary of 1000 generations represent the default setting in our scheme. Since genetic operators tend to be problem specific (Man et al., 1999), using the fixed parameters $N_p = 120$ and $r_e = 0.1$ we will examine

Table III. Methods taken for comparison with the proposed GA-WVDF framework.

Notation	Method	Reference
MF	Component-wise median filter	Zheng et al. (1993)
VMF	Vector median filter	Astola et al. (1990)
BVDF	Basic vector directional filter	Trahanias et al. (1996)
DDF	Directional-distance filter	Karakos and Trahanias (1997)
GVDF	Generalized vector directional filter	Plataniotis and Venetsanopoulos (2000)
SMF	Spherical median filter	Trahanias et al. (1996)
HVF	Hybrid vector filter	Gabbouj and Cheickh (1996)
WVDF	WVDF with $\mathbf{w} = [1,2,1,4,5,4,1,2,1]$	Lukac (2004)
LWVDF	Linearly optimized WVDF	Lukac et al. (2004a)
SWVDF	Sigmoidally optimized WVDF	Lukac et al. (2004a)

Figure 17. Test color images: (a) original image Parrots, (b) image Parrots corrupted by 5% impulsive noise ($p_v = 0.05$). [Color figure can be viewed in the online issue, which is available at www.interscience.wiley.com]

the influence of the probabilities p_c and p_m, and the number of generations on the aforementioned evaluation criteria.

Figure 11a demonstrates the dependence of the GA's cost (17) on the setting of the probabilities $p_c = 0.1, 0.2, \ldots, 0.9$ and $p_m = 0.05, 0.15, \ldots, 0.95$. To follow the standard practice in testing stochastic methods, 20 runs for each allowed combination of p_c and p_m were used. Figure 11a depicts the cost values averaged over 20 measurements. As it was expected, a large value of p_m extends the variability of individuals. Moreover, visual inspection of the corresponding standard deviation (Fig. 11b) reveals that the final values of the GA's cost function vary significantly. To this end, the largest spread of the cost values was observed for $p_c = 0.5$ and $p_m = 0.95$, whereas the $p_c = 0.5$ and $p_m = 0.45$ setting corresponded to the smallest deviation in the GA's cost values. The smallest averaged GA's cost was obtained using $p_c = 0.7$ and $p_m = 0.05$; therefore, this setting is used in the following experimentation.

Figure 12 allows for the comparison of the GA's convergence obtained using the default setting (single-point crossover and Gaussian mutation) and the conventional setting (arithmetic-point crossover and Gaussian mutation). The use of the arithmetic crossover (Fig. 12b) provides more uniform curves, and the convergence is usually obtained within 50 generations compared to 90 generations in the default setting (Fig. 12a). When these generations are reached, the convergence process continues significantly slower.

Figure 13 displays the best fitness values obtained using the parameters $p_c = 0.7$ and $p_m = 0.05$. Note that the curves are plotted for a single run in which the largest value of (13) among 20 runs was observed. Both settings resulted in the identical maximum fitness $\xi_{max} = 0.9937$. As it can be seen, in order to obtain the maximum fitness, 605 generations were needed using the default setting, whereas the use of the other setting led to the same value performing 864 generations during evolution.

The following experimentation was performed using the default setting only. Figure 14 plots the number of generations needed in order to obtain the best fitness. Note that 20 runs for each combination of p_c and p_m were executed. Visual inspection of the results reveals that the GA converges to the best solution slower for large p_m with small p_c. Figure 15 demonstrates that in many situations the final fitness increases with the number of generations. It should be mentioned that the MAE values (detail-preserving capability) are extremely small. Similar statements can be drawn using the NCD criterion (color preservation capability). In some cases, the improvement in terms of the MSE values (noise suppression capability) is not as high as it was expected. This behavior can be attributed to: (i) the utilization of the MAE-based optimization criterion in (17), and (ii) mainly to the fact that the GA did not converge to the solution that provides the best balance between the various objective measures.

Figure 16 shows zoomed parts of images achieved during the training. The visual quality of the output image, especially in terms of signal-detail preservation and color appearance, increases with

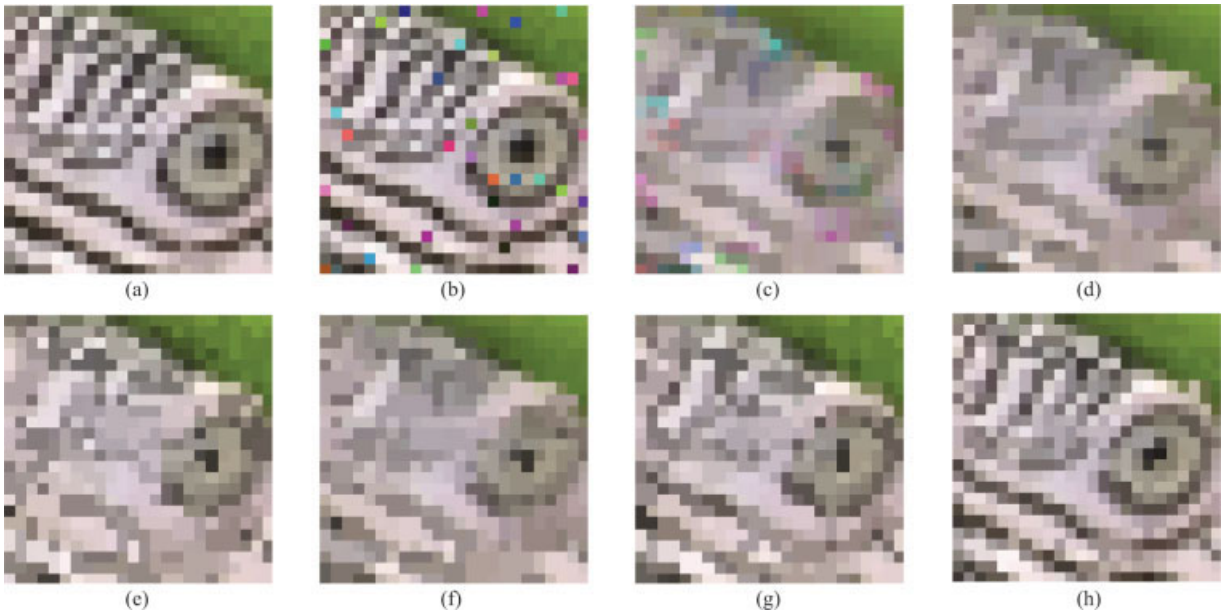

Figure 18. Zoomed results corresponding to Figure 17: (a) original image, (b) image corrupted by 5% impulsive noise ($p_v = 0.05$), (c) MF output, (d) VMF output, (e) BVDF output, (f) DDF output, (g) LWVDF output, (h) proposed filter ($\mathbf{w}_1$) output optimized using Figure 8. [Color figure can be viewed in the online issue, which is available at www.interscience.wiley.com]

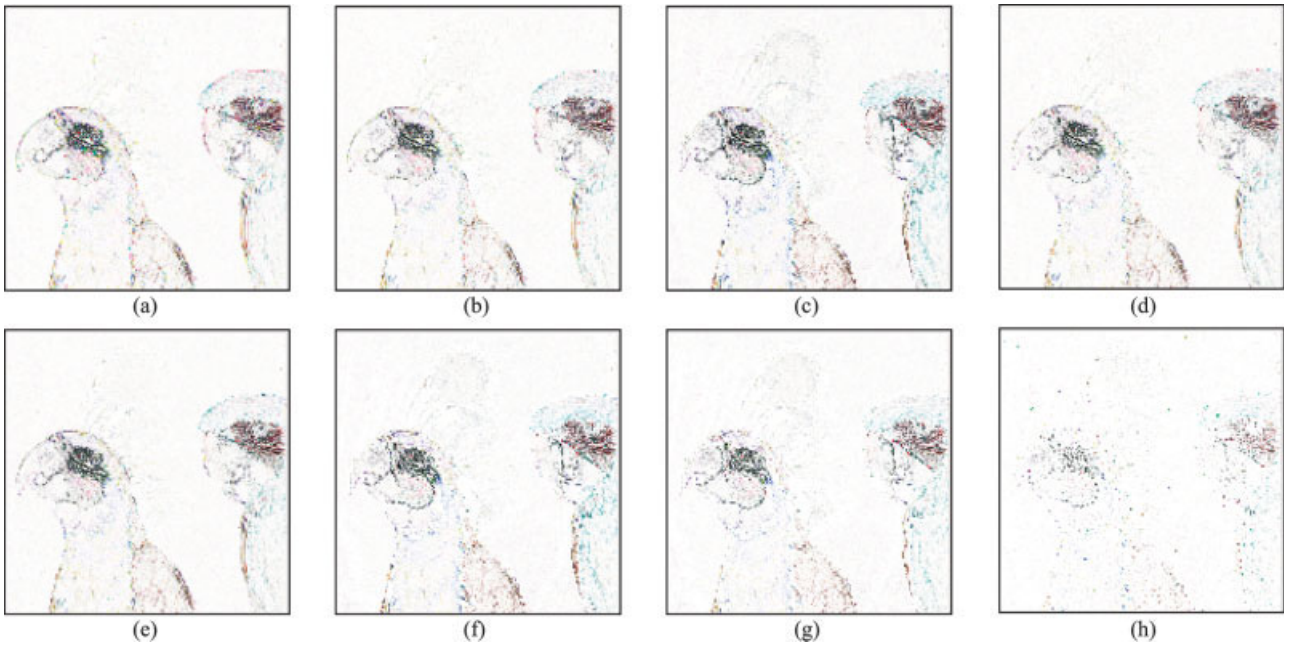

Figure 19. Estimation errors emphasized by a factor of 2.5 corresponding to Figure 17: (a) MF output, (b) VMF output, (c) BVDF output, (d) DDF output, (e) HVF_1 output, (f) nonadaptive WVDF with $\mathbf{w} = [1,2,1,4,5,4,1,2,1]$, (g) LWVDF output, (h) proposed filter ($\mathbf{w}_1$) output optimized using Figure 8. [Color figure can be viewed in the online issue, which is available at www.interscience.wiley.com]

the number of generations. It can be seen that this improvement also results in improved objective quality measures listed in the description of Figure 16.

Table I shows the weight vectors obtained using the WVDF framework. The least mean error principle solutions (Lukac et al., 2004) with the linear (LWVDF) and sigmoidal (SWVDF) approximation of the sign function as well as the proposed GA-optimized WVDF were obtained using identical images depicted in Figure 8. Note that the vector $\mathbf{w}_1$ corresponds to the best fitness obtained for $p_c = 0.7$ and $p_m = 0.05$ used in Figure 13. The vector $\mathbf{w}_2$ consists of the weights averaged over the best solutions obtained for each of 20 different runs (1000 generations) of the GA and the individual settings of $p_c = 0.1, 0.2, \ldots, 0.9$ and $p_m = 0.05, 0.15, \ldots, 0.95$. Finally, $\mathbf{w}_3$ contains the weighting coefficients obtained under a procedure identical to the one used in determining $\mathbf{w}_2$. The only difference is that the best solutions were achieved within 10 generations, instead of 1000 generations, needed in the determination of $\mathbf{w}_2$. These results confirm our expectations that the center sample has the greatest impact on the accuracy of the estimates when impulsive noise is corrupting the original input. In general, the contribution of the surrounding color vectors is approximately five times smaller compared with the contribution of the central sample.

Table II illustrates the influence of the evolution process. Since both $\mathbf{w}_2$ and $\mathbf{w}_3$ are calculated over 1800 measurements (20 runs, 9 values of p_c, and 10 values of p_m), the influence of the number of generations on the uniformity (or variability) of the winning chromosomes can be evaluated. Table II summarizes the standard deviation corresponding to the individual weights of $\mathbf{w}_2$ and $\mathbf{w}_3$. The results demonstrate that (i) winning chromosomes obtained within 10 generations (for vector $\mathbf{w}_3$) vary significantly within the set of all obtained solutions, and (ii) GA did not achieve globally optimal solutions in many cases. Please note that the weight w_5 corresponding to the central sample $\mathbf{x}_{(N+1)/2} = \mathbf{x}_5$ was observed to be the most consistent value within $\mathbf{w}_3$. However, if 1000 generations are used to obtain GA evolution, the process converges to similar solutions (globally optimal or close weight vectors); and thus, the averaged weight vector $\mathbf{w}_2$ does not deviate significantly from the sets of 1800 measurements. Since neighboring vectors do not have a large impact on the WVDF output, the lowest consistency in the obtained weights corresponds to the central weight w_5.

In the sequence, the GA-optimized WVDF filters are compared in terms of performance, to the color image filters listed in Table III. To facilitate the comparison, widely used test images such as the Lena image (Fig. 8a) and the Parrots image (Fig. 17a) are utilized. These standard size (256×256) images are displayed using 8-bit per channel RGB representation. To measure similarity between the original RGB image $\mathbf{o}$ and the filtered image $\mathbf{y}$, and determine objectively the quality of filtered images, we will make use of the

Table IV. Comparison of the presented algorithms using impulsive noise corruption $p_v = 0.02$.

	Lena			Parrots		
Method	MAE	MSE	NCD	MAE	MSE	NCD
Noisy	1.519	173.0	0.0180	1.578	186.2	0.0177
MF	3.239	45.9	0.0414	2.547	57.9	0.0150
VMF	3.300	47.8	0.0391	2.493	58.0	0.0123
BVDF	3.694	55.1	0.0394	3.289	101.8	0.0106
DDF	3.379	48.8	0.0389	2.482	60.2	0.0108
GVDF	3.587	55.3	0.0420	2.864	84.8	0.0117
SMF	3.523	45.6	0.0406	2.896	57.4	0.0120
HVF	3.450	48.4	0.0397	2.604	59.8	0.0114
WVDF	2.487	36.0	0.0265	1.879	53.3	0.0059
LWVDF	1.790	23.7	0.0211	1.306	28.8	0.0060
SWVDF	1.631	18.5	0.0172	1.433	45.2	0.0043
Proposed $\mathbf{w}_1$	0.849	12.4	0.0089	0.694	20.3	0.0025
Proposed $\mathbf{w}_2$	0.832	11.8	0.0087	0.696	20.7	0.0022
Proposed $\mathbf{w}_3$	1.094	13.6	0.0115	0.933	28.7	0.0028

Table V. Comparison of the presented algorithms using impulsive noise corruption $p_v = 0.05$.

Method	Lena			Parrots		
	MAE	MSE	NCD	MAE	MSE	NCD
Noisy	3.762	427.3	0.0445	3.805	443.6	0.0432
MF	3.394	49.7	0.0442	2.718	63.1	0.0170
VMF	3.430	50.8	0.0403	2.669	64.2	0.0132
BVDF	3.818	58.6	0.0407	3.460	109.0	0.0116
DDF	3.509	52.3	0.0402	2.645	65.3	0.0117
GVDF	3.587	55.3	0.0420	3.036	93.6	0.0126
SMF	3.523	45.6	0.0406	2.927	61.6	0.0130
HVF	3.857	56.9	0.0434	2.786	65.7	0.0122
WVDF	2.989	56.3	0.0314	2.061	62.2	0.0090
LWVDF	2.399	33.4	0.0256	2.029	63.5	0.0064
SWVDF	1.783	24.2	0.0188	1.574	50.4	0.0052
Proposed $\mathbf{w}_1$	1.084	24.8	0.0113	0.893	29.9	0.0035
Proposed $\mathbf{w}_2$	1.065	23.9	0.0111	0.893	29.9	0.0036
Proposed $\mathbf{w}_3$	1.278	21.7	0.0134	1.106	36.2	0.0038

Table VI. Comparison of the presented algorithms using impulsive noise corruption $p_v = 0.10$.

Method	Lena			Parrots		
	MAE	MSE	NCD	MAE	MSE	NCD
Noisy	7.312	832.0	0.0840	7.526	882.0	0.0857
MF	3.703	56.8	0.0489	2.960	70.0	0.0198
VMF	3.687	56.5	0.0428	2.890	69.6	0.0142
BVDF	4.099	67.6	0.0432	3.630	113.5	0.0127
DDF	3.733	57.3	0.0424	2.839	69.7	0.0128
GVDF	3.925	66.8	0.0448	3.188	96.2	0.0137
SMF	3.907	53.1	0.0439	3.133	67.1	0.0141
HVF	3.857	56.9	0.0434	3.002	69.9	0.0132
WVDF	2.989	56.3	0.0314	2.362	77.2	0.0083
LWVDF	2.661	42.5	0.0281	2.238	72.2	0.0074
SWVDF	2.114	39.8	0.0219	3.196	110.2	0.0108
Proposed $\mathbf{w}_1$	1.606	55.2	0.0162	1.340	59.4	0.0062
Proposed $\mathbf{w}_2$	1.605	59.2	0.0160	1.375	65.0	0.0063
Proposed $\mathbf{w}_3$	1.700	44.6	0.0173	1.418	52.9	0.0056

MAE, MSE, and NCD criteria defined by (14), (15), and (16), respectively.

Note that WVDF filters were primarily focusing on removing additive impulsive noise. Therefore, the test images have been corrupted by 2, 5, and 10% impulsive noise of (12) corresponding to impulsive noise probability of $p_v = 0.02$, $p_v = 0.05$, and $p_v = 0.10$ in (12), respectively. Since training data are unavailable in realistic applications, determining robustness of the proposed filters in mismatched operating conditions is of paramount importance.

Figure 18 illustrates the performance of the methods using enlarged parts of the test image Parrots. These results clearly indicate that the component-wise median filter (MF) produces color artifacts Figure 18c. It can be seen that standard vector filtering schemes, such as VMF, BVDF, and DDF, avoid color artifacts; however, VMF and DDF often produce regions called streaks (Figs. 18d and 18f) of constant or nearly constant brightness. It can be seen that the angular minimization approach employed by the BVDF is useful, and it leads to better performance (Fig. 18e) in terms of the color–structural preservation. The recently introduced linearly optimized WVDF (LWVDF) filter (Lukac et al., 2004a) exhibits improved detail-preserving characteristics and produces an output image (Fig. 18g), which is close to the original image shown in Figure 18a. The proposed genetically optimized filtering framework produces an output image (Fig. 18h), which looks sharper than Figure 18g. Moreover, the GA-WVDF output is characterized by excellently preserved color and structure elements. These excellent characteristics result in the smallest estimation error (Fig. 19) among tested filters, as can be seen from the results summarized in Tables IV–VI. These results demonstrate that the proposed optimal filter works well using the training image, although the amount of image corrupting noise (here impulsive noise) encountered during the actual operation, differs significantly from the amount assumed present during training. Moreover, the solution is stable and robust even when during the actual operation an image such as Parrots, with significantly different characteristics, both in color and structural information, from the one used in training, is encountered. This suggests that the optimal GA-WVDF framework constitutes a robust solution for the removal of outliers and impulsive noise.

The following experimentation examines the performance of the optimal GA-WVDF filters in different qualitative and quantitative noise environments. During the actual operation, the noisy inputs are real images corrupted by real, nonapproximated noise, which is different in characteristics and statistical properties from the impulsive noise assumed during training. Figure 20 shows a digitized artwork and a television image. Noise is introduced into the digitized artworks by scanning damaged and granulated surfaces of the original paintings, mural frescos, and roll documents. Noise is also introduced into television images, mostly due to atmospheric interference and imperfections of the transmission channel. Since the original, noise-free images are not available, the images shown in Figures 21 and 22 are subjectively evaluated. Image quality is evaluated with respect to the structural content (edges, textures, and fine details) preservation, and the presence of residual noise or color artifacts as a result of faulty processing. Note that the human visual system is sensitive to changes in color and thus maintaining the sharpness of the edges is as important as removing the image noise when it comes to the visual assessment of the filtering process. Edges are important features since they provide an indication of the shape of the objects in the image.

The VMF technique exhibits robust noise-attenuation characteristics; however, it removes important color/structural details (Figs. 21b and 22b). The BVDF enhanced images shown in (Figs. 21c and 22c) look sharper and with more details, compared with the VMF obtained outputs. However, the proposed method provides the best

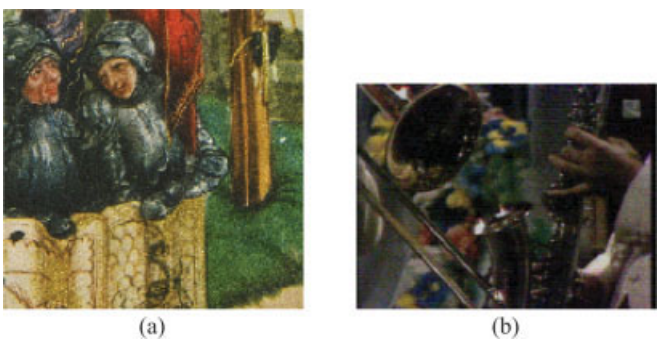

Figure 20. Real images: (a) digitized image of fine arts, (b) television image. [Color figure can be viewed in the online issue, which is available at www.interscience.wiley.com]

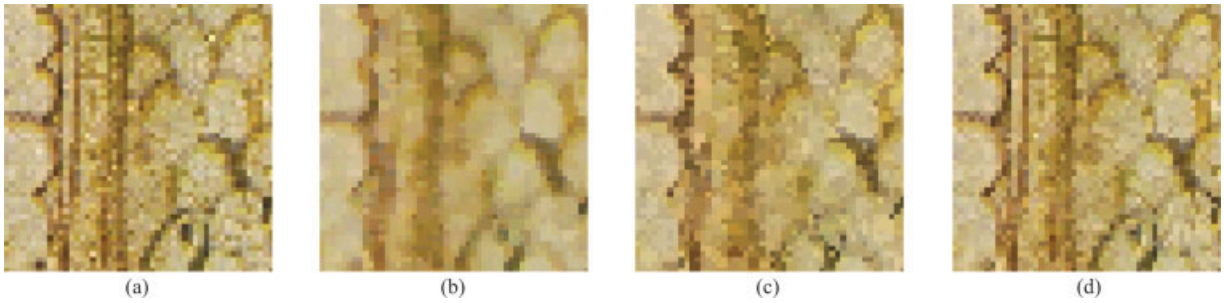

Figure 21. Zoomed results corresponding to Figure 20a: (a) original image, (b) VMF output, (c) BVDF output, (d) proposed filter ($\mathbf{w}_1$) output optimized using Figure 8. [Color figure can be viewed in the online issue, which is available at www.interscience.wiley.com]

results in terms of subjective evaluation, since the corresponding images shown in Figures 21d and 22d contain all the important details. The GA-based solution is capable of removing samples deviating from their neighbors while excellently preserves color/structural information. This suggests that the filter is sufficiently robust to relatively large deviations from the conditions assumed during training. However, it should be noted that in case of substantial qualitative difference in terms of noise characteristics, Gaussian versus impulsive, there is a drop in performance, which largely depends on the intensity of the corrupting noise. In this case, reoptimization of the filter coefficients may be recommended. It should be emphasize that selection type filters, such as the considered WVDF, are primarily geared to address to the problem of impulsive noise removal. For such a task, the proposed solution holds excellent performance.

Summarizing the results presented earlier, the following conclusions can be drawn:

- The presented GA-WVDF framework blends together concepts from evolutionary computation, nonlinear estimation theory, multichannel image processing, and it can be readily applied to emerging application areas, such as color image processing and virtual restoration of artworks. The results and improvements presented in the paper clearly demonstrate that from a practical point of view, the proposed GA optimization-based filtering solution delivers excellent performance.
- The GA-WVDF solution is sufficiently robust, attenuates impulsive noise present in color images, and produces images with excellent fidelity compared to the originals.
- The GA-WVDF optimization process converges to a useful suboptimal solution within 100 generations. The uniformity of the optimal WVDF weight vectors obtained for the different parameters p_c and p_m increases with the number of generations. The smallest standard deviation in the GA-WVDF convergence was observed for $p_c = 0.5$ and $p_m = 0.45$. The parameters $p_c = 0.7$ and $p_m = 0.05$ were found to produce the smallest cost (averaged over 20 runs) of the GA-WVDF optimization process for all settings of the parameters p_c and p_m considered here. The maximum fitness 0.9937 was obtained for the parameters $p_c = 0.7$ and $p_m = 0.05$.
- The optimal GA-WVDF filters are consistent in performance even when the image corrupting noise differs quantitatively from the assumed during training noise model. Moreover, the proposed method outperforms other techniques in terms of the most commonly used image quality measures. Optimized WVDF filters are capable of preserving the color/structural information of real images, such as digitized artworks and television images, while attenuating low-level noise appearing in forms of impulsive sequences or isolated deviating colors.

VII. CONCLUSIONS

This study introduced a new, genetically optimized color image filtering solution operating on nonnegative real weights and the directionality of color vectors. The proposed GA optimization concept significantly improves color/structural preserving characteristics of the traditional color filtering schemes, while exhibiting acceptable noise attenuation capabilities. The behavior of the introduced framework was analyzed in detail and modifications of the proposed framework have been provided as well. Television image enhancement and virtual restoration of artworks were introduced as an

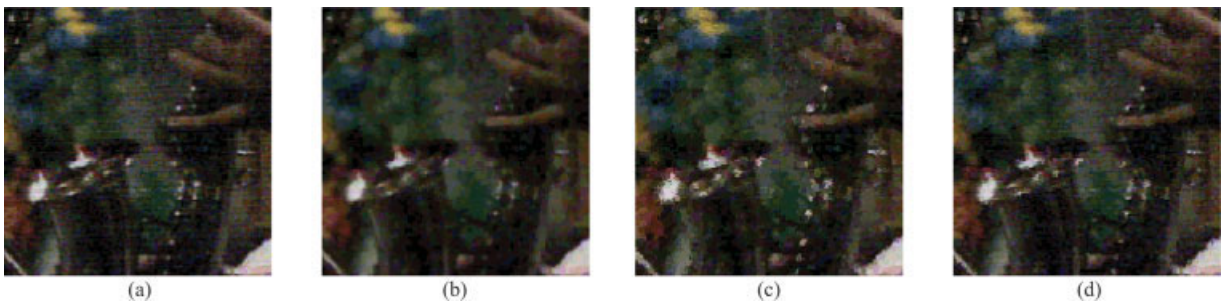

Figure 22. Zoomed results corresponding to Figure 20b: (a) original image, (b) VMF output, (c) BVDF output, (d) proposed filter ($\mathbf{w}_1$) output optimized using Figure 8. [Color figure can be viewed in the online issue, which is available at www.interscience.wiley.com]

example of emerging applications in color image filtering. Simulation results and comparisons reported here indicate that the proposed framework achieves excellent trade-off between smoothing and preserving characteristics, and is sufficiently robust and can outperform the commonly used color image filtering schemes in terms of both objective and subjective image quality measures.

REFERENCES

J. Arabas and S. Kozdrowski, Applying an evolutionary algorithm to telecommunication network design, IEEE Trans Evol Comput 5 (2001), 309–322.

J. Astola, P. Haavisto, and Y. Neuvo, Vector median filters, Proc IEEE 78 (1990), 678–689.

I. Avcibas, B. Sankur, and K. Sayood, Statistical evaluation of image quality measures, J Electron Imaging 11 (2002), 206–223.

H.G. Beyer and K. Deb, On self-adaptive features in real-parameter evolutionary algorithms, IEEE Trans Evol Comput 5 (2001), 250–270.

P.A.N. Bosman and D. Thierens, The balance between proximity and diversity in multiobjective evolutionary algorithms, IEEE Trans Evol Comput 7 (2003), 174–188.

M. Brameier and W. Banzhaf, A comparison of linear genetic programming and neural networks in medical data mining, IEEE Trans Evol Comput 5 (2001), 17–26.

D. Chen, T. Aoki, N. Homma, T. Terasaki, and T. Higuchi, Graph-based evolutionary design of arithmetic circuits, IEEE Trans Evol Comput 6 (2002), 86–100.

D. Dasgupta, G. Hernandez, and F. Nino, An evolutionary algorithm for fractal coding of binary images, IEEE Trans Evol Comput 4 (2000), 172–181.

O. Faugeras, Digital color image processing within the framework of a human visual model, IEEE Trans Acoust Speech Signal Process 27 (1979), 380–393.

Y. Fujiwara and H. Sawai, Evolutionary computation applied to mesh optimization of a 3-D facial image, IEEE Trans Evol Comput 3 (1999), 113–123.

M. Gabbouj and A. Cheickh, Vector median-vector directional hybrid filter for color image restoration, Proceedings of European signal Processing Conference, EUSIPCO-96, Trieste, Italy, 1996, pp. 879–881.

D. Goldberg, Genetic algorithms in search, optimisation, and machine learning, Addison-Wesley, Reading, MA, 1989.

D. Goldberg, The design of inovation: Lessons from and for competent genetic algorithm, Kluwer Academic Publishers, Boston, 2002.

M.S. Hamid, N.L. Harvey, and S. Marshall, Genetic algorithm optimization of multidimensional grayscale soft morphological filters with applications in film archive restoration, IEEE Trans Circuits Syst Video Technol 13 (2003), 406–416.

D.G. Karakos and P.E. Trahanias, Generalized multichannel image-filtering structure, IEEE Trans Image Process 6 (1997), 1038–1045.

L. Khriji and M. Gabbouj, Vector median-rational hybrid filters for multichannel image processing, IEEE Signal Process Lett 6 (1999), 186–190.

K.S. Leung, Q.H. Duan, Z.B. Xu, and C.K. Wong, A new model of simulated evolutionary computation: Convergence analysis and specifications, IEEE Trans Evol Comput 5 (2001), 3–16.

R.S. Lin and Y.C. Hsueh, Multichannel filtering by gradient information, Signal Process 80 (2000), 279–293.

J. Liu, Y. Tang, and Y.C. Cao, An evolutionary autonomous agents approach to image feature extraction, IEEE Trans Evol Comput 1 (1997), 141–156.

L. Lucat, P. Siohan, and D. Barba, Adaptive and global optimization methods for weighted vector median filters, Signal Process: Image Commun 17 (2002), 509–524.

R. Lukac, Adaptive vector median filtering, Pattern Recogn Lett 24 (2003), 1889–1899.

R. Lukac, Adaptive color image filtering based on center-weighted vector directional filters, Multidimensional Syst Signal Process 15 (2004), 169–196.

R. Lukac, K.N. Plataniotis, and B. Smolka, Genetic optimization of weighted vector directional filters, Proceedings of the 9th International Workshop on Systems, Signals and Image Processing Prague, Czech Republic, September 10–11, 2003b, pp. 5–9.

R. Lukac, K.N. Plataniotis, B. Smolka, and A.N. Venetsanopoulos, Weighted vector median optimization, Proc. 4th EURASIP Conference focused on Video/Image Processing and Multimedia Communications 1 (2003a), 227–232.

R. Lukac, K.N. Plataniotis, B. Smolka, and A.N. Venetsanopoulos, Color image filtering and enhancement based on genetic algorithms, Proc IEEE Int Symp Circuits Syst 3 (2004b), 913–916.

R. Lukac, K.N. Plataniotis, B. Smolka, and A.N. Venetsanopoulos, Generalized selection weighted vector filters, EURASIP 2004, J Appl Signal Process 12 (2004c), 1870–1885. Special issue on Nonlinear Signal and Image Processing.

R. Lukac, K.N. Plataniotis, B. Smolka, and A.N. Venetsanopoulos, A multichannel order-statistic technique for cDNA microarray image processing, IEEE Trans Nanobiosci 3 (2004d), 272–285.

R. Lukac, K.N. Plataniotis, B. Smolka, and A.N. Venetsanopoulos, cDNA microarray image processing using fuzzy vector filtering framework, Fuzzy Sets Syst 152(1) (2005b), 17–35. Special issue on Fuzzy Sets and Systems in Bioinformatics.

R. Lukac, B. Smolka, K. Martin, K.N. Plataniotis, and A.N. Venetsanopulos, Vector filtering for color imaging, IEEE Signal Processing Magazine, Special Issue on Color Image Processing 22 (2005a), 74–86.

R. Lukac, B. Smolka, K.N. Plataniotis, and A.N. Venetsanopulos, Selection weighted vector directional filters, Comput Vis Image Understand, 94(1–3) (2004a), 140–167. Special issue on Colour for Image Indexing and Retrieval.

R. Lukac, B. Smolka, A. Swierniak, K.N. Plataniotis, and A.N. Venetsanopoulos, Weighted vector directional filters optimized by genetic algorithms, Proceedings of the 5th International Conference on Parallel Processing and Applied Mathematics Czestochowa, Poland, September 7–10, 2003c, pp. 595–600.

K.F. Man, K.S. Tang, and S. Kwong, Genetic algorithms: Concept and design, Springer Verlag, London, 1999.

S. Mitra and J. Sicuranza, Nonlinear image processing, Academic Press, New York, 2001.

N. Nikolaidis and I. Pitas, Nonlinear processing and analysis of angular signals, IEEE Trans Signal Processing 46 (1998), 3181–3194.

R.S. Parpinelli, H.S. Lopes, and A.A. Freitas, Data mining with an ant colony optimization algorithm, IEEE Trans on Evol Comput 6 (2002), 321–332.

I. Pitas and A.N. Venetsanopoulos, Nonlinear digital filters, principles and applications, Kluwer Academic Publishers, Boston, 1990.

K.N. Plataniotis, D. Androutsos, and A.N. Venetsanopoulos, Adaptive fuzzy systems for multichannel signal processing, Proc IEEE 87 (1999), 1601–1622.

K.N. Plataniotis and A.N. Venetsanopoulos, Color image processing and applications, Springer Verlag, Heidelberg, 2000.

J.C. Principe, N.R. Euliano, and W.C. Lefebrre, Neural and adaptive systems: Fundamentals through simulation, Wiley, New York, 1999.

H. Rantanen, M. Karlsson, P. Pohjala, and S. Kalli, Color video signal processing with median filters, IEEE Trans Consumer Electron 38 (1992), 157–161.

M. Russo, Genetic fuzzy learning, IEEE Trans Evol Comput 4 (2000), 259–273.

B. Smolka, R. Lukac, A. Chydzinski, K.N. Plataniotis, and K. Wojciechowski, Fast adaptive similarity based impulsive noise reduction filter, RealTime Imaging 9(4) (2003), 261–276. Special issue on Spectral Imaging.

M. Szczepanski, B. Smolka, K.N. Plataniotis, and A.N. Venetsanopoulos, On the geodesic paths approach to color image filtering, Signal Process 83 (2003), 1309–1342.

K. Tang, J. Astola, and Y. Neuvo, Nonlinear multivariate image filtering techniques, IEEE Trans Image Process 4 (1995), 788–798.

B. Tang, G. Sapiro, and V. Caselles, Color image enhancement via chromaticity diffusion, IEEE Trans Image Process 10 (2001), 701–707.

H.H. Tsai and P.T. Yu, Genetic-based fuzzy hybrid multichannel filters for color image restoration, Fuzzy Sets Syst 114 (2000), 203–224.

P.E. Trahanias, D. Karakos, and A.N. Venetsanopoulos, Directional processing of color images: Theory and experimental results, IEEE Trans Image Process 5 (1996), 868–881.

M.I. Vardavoilia, I. Andreadis, and P. Tsalides, A new vector median filter for color image processing, Pattern Recogn Lett 22 (2001), 675–689.

T. Viero, K. Oistamo, and Y. Neuvo, Three-dimensional median related filters for color image sequence filtering, IEEE Trans Circuits Syst Video Technol 4 (1994), 129–142.

G. Wyszecki and W.S. Stiles, Color science: Concepts and methods, quantitative data and formulas, 2nd Edition, Wiley, New York, 1982.

J. Zheng, K.P. Valavanis, and J.M. Gauch, Noise removal from color images, J Intell Robotic Syst 7 (1993), 257–285.